ISSN (Online) 2394-6849

International Journal of Engineering Research in Electronics and Communication Engineering (IJERECE)
Vol 5, Issue 4, April 2018

Segmentation of Fluid Regions in Patients Having Diabetic Macular Edema Using Graph Algorithm and Neutrosophic Sets In Optical Coherence Tomography Images

[1] Anupriya.G, [2] Usha.A
[2] Associate Professor
[1][2] Easwari Engineering College, Chennai

Abstract: **- Optical coherence tomography (OCT) is a latest imaging technology with applications in medicine, biology as well as materials investigations. Over the time, diabetes can lead to serious problems in the blood vessels, retina, nerves, brain and eyes. These problems can lead to Diabetic macular edema (DME) causing problem in eye area to resolve this, Segmentation of fluid in optical coherence tomography images is implemented. Segmentation of OCT images is done using neutrosophic set and graph algorithm. Graph algorithm is applied to the neutrosophic set in order to segment the inner layers of eye and identify the fluid regions. Cluster computation is done using the cost function method to implement cluster based fluid segmentation. Finally, by ignoring the very small regions and middle layers finally the fluid regions are obtained for the diagnosis of DME.**

***KEYWORDS*- Fluid/cyst segmentation, graph algorithm, neutrosophic set, optical coherence tomography, diabetic macular edema.**

I. INTRODUCTION

Diabetic macular edema (DME) is a consequence of microvascular changes in the retina that develop because of diabetic retinopathy. In DME, weakened capillaries present in the eye allow the fluid to cross over the blood-retinal barrier, which in turn results in retinal thickening and accumulation of fluid in the retinal tissue of the macula. Patients suffering from DME mostly experience blurred vision, floaters and dark areas in the visual field, and poor night vision. Untreated, DME causes moderate vision loss in 25-30% of patients, and severe vision loss and blindness in many individuals The economic impact of DME and its treatment is also substantial. Findings from a recent study indicate that the patients with DME consume more resources overall than patients with diabetes who do not have DME, resulting in significantly higher direct Medicare. The Neutrosophic components are categorized as True(T), Intermediate(I), False(F) therefore represents the membership, indeterminacy, and non-membership values respectively, Hence [- 0, 1+] is the non-standard unit interval, and thus this explains the neutrosophic set. Neutrosophic set are applicable in mathematics, physics and philosophy. Finally, the introduction of the neutrosophic set operations in (complement, intersection, union, difference, Cartesian product, inclusion, and n-ary relationship), some generalizations, and after process the distinctions between the neutrosophic set and the intuitionistic fuzzy set is explored. Shortest path analysis is to identify the blood vessels in retinal images. So, the shortest path between every pair of pixels (where speed through a pixel is proportional to the gray level) could be found, and then the counter is increased for every pixel on the path. Once all pixel paths through a pixel have been counted, the highest counts should correspond to vessel pixels. However, this has exponential complexity in the number of pixels. At last, not all pixel pairs can be analyzed. So to investigate the small subset of pixels to speed the process, and propose two methods such that the curl method, and polynomial method. The advantages and limitations of approaches for addressing these research questions using the path-level movement data, and present general guidelines for choosing methods is based on data characteristics and questions. The diversity of available path segmentation approaches as well as indicates the need for studies which compare the utilization of different methods, and identifies opportunities for future developments in path-level data analysis. “Many people believe that assigning the exact number to an expert’s opinion is too restrictive, and the assignment of an interval of values is more realistic” which is exactly similar to the imprecise probability theory, where instead of a crisp

ISSN (Online) 2394-6849

International Journal of Engineering Research in Electronics and Communication Engineering (IJERECE)
Vol 5, Issue 4, April 2018

probability one has an interval (upper and lower) probabilities from decision making and control theory (making a decision, not making, or hesitating), from accepted/rejected/pending, etc. and guided by the fact that the law of excluded middle did not work any longer in the modern logics, Therefore combined the non-standard analysis.

II. RELATED WORK

For fluid/cyst segmentation, first the OCT image is transformed into NS by the proposed method. This method not only transforms the image into NS but also changes the gray level of the noisy pixels. In NS, indeterminacy is one of the important concepts, and in the image processing domain, it is interpreted as noise. Here, a new definition of indeterminacy is proposed. In the basic NS-based image segmentation method, indeterminacy set. ROI segmentation with shortest path graph Fluid/cyst regions are all located between ILM and RPE layers in the OCT images of DME subjects. Therefore, the first step of our proposed method is the segmentation of these layers as the ROI in the NS domain. This step is very important due to two aspects. First, the background region is very similar to fluid/cyst regions in both brightness and texture. This can easily mislead the segmentation method since this method is based on an unsupervised clustering scheme and will be affected by the similarity between the desired fluid/cyst regions and the irrelevant background region. The second reason for ROI segmentation is speeding up since the ROI is processed instead of the whole image. the image to one node in a graph. To consider the local relationship between pixels. Therefore, by considering the local relationship for neighbors of each pixel, the 8-regular graph is constructed. For segmentation, the image is first filtered with filter H for the calculation of vertical gradient of each pixel. Segmentation scheme for fluid/cyst regions, an unsupervised clustering method is proposed for the segmentation of fluid/cyst regions in OCT images. For this task, a new cost function is proposed. Although the OCT images were denoised, in the clustering scheme, the effect of noise is still considered in the proposed cost function in two steps. In the first one, an extra cluster referred as noise cluster (NC) is considered beside K main clusters. Therefore, it is expected that the noisy pixels will be assigned to the NC. The second step is that the indeterminacy of the pixels is included in the cost function.

Post processing with middle layers segmentation the proposed post-processing is an important step in image segmentation. After segmentation with the proposed clustering scheme, some segmented regions are incorrectly marked as fluid/cyst. The regions between OPL and ISM are similar to fluid/cyst regions in both texture and brightness. In the proposed approach, another layer segmentation method for OPL and ISM segmentation is proposed which is similar to the proposed ROI segmentation method and is based on the graph shortest path algorithm. Images were analyzed and we found that for images with a great deal of fluid/cyst, ophthalmologists are interested in the segmentation of the image with more general and bigger segments. Therefore, segmentation with a small K has the best correlation with the segmentation annotated by an ophthalmologist. For the images with smaller fluid/cyst regions, a larger K is more appropriate. By this interpretation, an automated method is proposed for determining K. The goal of the layer segmentation method is to avoid false positives in fluid/cyst segmentation, and not to segment layers that correlate well with annotations by the ophthalmologist. Therefore, segmented sub-retinal layers have different positions as compared with segmented layers by the ophthalmologist and these are not comparable.

III. PROPOSED WORK

The proposed fluid/cyst segmentation method has been evaluated with respect to dice coefficient, precision and sensitivity criteria. Accuracy and specificity criteria haven't been used here since these are biased to very high values (close to 100%). This is due to the large number of negative (non-fluid) pixels and the large number of true negative (TN) segmented pixels. A clustering method is proposed for the segmentation of fluid/cyst regions in OCT images. For this task, a new cost function is proposed. Although the OCT images were denoised, in the clustering scheme, the effect of noise is still considered in the proposed cost function in two steps. In the first one, an extra cluster referred as noise cluster (NC) is considered beside K main clusters. Therefore, it is expected that the noisy pixels will be assigned to the NC.

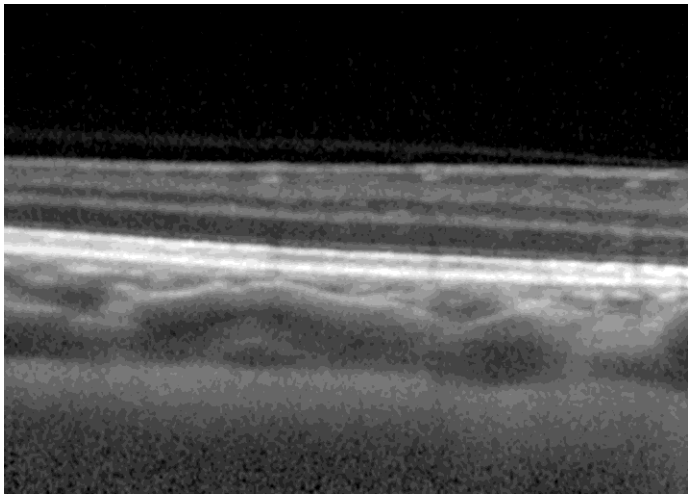

Figure 6.1 OCT Image

ISSN (Online) 2394-6849

International Journal of Engineering Research in Electronics and Communication Engineering (IJERECE)
Vol 5, Issue 4, April 2018

- PREPROCESSING
- ROI EXTRACTION
- SEGMENTATION

1. Image database acquisition and Tool

The local UMN DME dataset and the segmented images of the approach presented in this paper for the UMN and Optima data sets.

2. Preprocessing

Consider the huge number of components that influence the quality and appearance of a light microscope image:

- Microscope optics acquainting contortions with a picture if not appropriately utilized.
- Environmental conditions influencing the morphology of cells in culture and during handling
- Fixatives bringing about some morphological twisting and differential extraction of components
- Labeling that is uneven or lopsided, or improper decision of labels
- Different filter sets giving differing perspectives of fluorescent indicators
- Photo bleaching of fluorescent dyes
- Uneven illumination
- Visual observation not matching the linear reaction of a camera
- Instrumental twists (fixed bias pattern noise and electrical interference)

3. Segmentation

Taking after the pre-processing stage, the image is segmented in a process that concentrates paramount data and traits from the histology image. Segmentation divides an image into multiple components and is usually employed to distinguish targets or other relevant info in digital pictures such as organs, tissue components. This research utilizes breast histology images and the tissue image consists of the background, storm, luminal cytoplasm and nuclei. The segmentation system connected to the histology image must have the capacity to recognize and concentrate the storm, luminal and nuclei from the background. A multistage segmentation strategy is obliged to fragment each one cell and other regions from the breast histology image. With a specific end goal to correctly extricate the peculiarities of a cell, the segmentation methodology obliges thought of a pathologist's learning and mediation to demonstrate the gimmicks generally utilized for breast histology determination, for instance, the relationship between the cell gimmicks and the sort and example of an ailment. In this research scale space, based region growing and k – means clustering method has been utilized to separation breast histology image into distinctive areas, e.g. cell, luminal region, cytoplasm, storm and the background. The proposed weight computation between any two arbitrary pixels (a_1,b_1) and (a_2,b_2) is defined by

$W((a_1,b_1),(a_2,b_2)) = 4 \times MaxG - V\ erGrad(a_1,b_1) - V\ erGrad(a_2,b_2) + 2 \times mean(R)$ where MaxG is the maximum gray level of the image and R is a set of D pixels above (a1,b1). In all experiments, D is set to 40. Based on the filter H, the maximum of VerGrad is 2 × MaxG. So, the maximum of V erGrad(a1,b1) + $V\ erGrad(a_2,b_2)$ is 4 × $MaxG$VerGrad(a2,b2) is 4 × MaxG

The first step in normal analysis is to extract characteristic features from mammogram images. From the perspective of pattern classification, feature extraction is a very important step in that the ultimate performance of the system is not determined by optimal parameters of the classifier, but by the intrinsic separability of the feature vectors. The characterization of normal tissue poses a real challenge due to the complications in the normal tissues and the normal mammogram is not well defined. Certain subtle breast cancers cannot be easily distinguished from the surrounding normal tissue. Therefore the heterogeneous nature of different breast cancers of different sizes also poses real challenges for the purpose of feature extraction. In this method describe several feature sets can be used to separate normal and the abnormal regions. All our features are extracted from 512 X 512 regions of mammogram.

IV. RESULTS AND DISCUSSIONS

A clustering method is proposed for the segmentation of fluid/cyst regions in OCT images. For this task, a new cost function is proposed. Although the OCT images were denoised in Algorithm, in the clustering scheme, the effect of noise is still considered in the proposed cost function in two steps. In the first one, an extra cluster referred as noise cluster (NC) is considered beside K main clusters. Therefore, it is expected that the noisy pixels will be assigned to the NC.

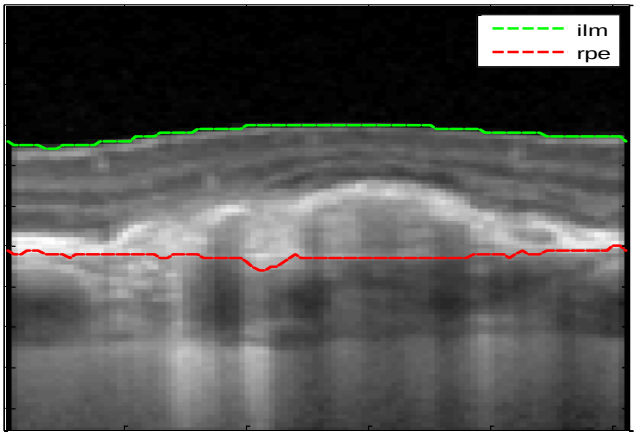

Figure 6.2 Fluid/cyst segment Region

ISSN (Online) 2394-6849

International Journal of Engineering Research in Electronics and Communication Engineering (IJERECE)
Vol 5, Issue 4, April 2018

The proposed fluid/cyst segmentation has been tested on the three mentioned datasets. The final fluid/cyst segmentation results on Duke, Optima and local UMN datasets are illustrated in Figs. 6.4, 6.5 and 6.6. The proposed fluid/cyst segmentation method has been evaluated with respect to dice coefficient, precision and sensitivity criteria. Accuracy and specificity criteria haven't been used here since these are biased to very high values (close to 100%). This is due to the large number of negative (non-fluid) pixels and the large number of true negative (TN) segmented pixels. Segmentation results of our proposed method using Duke dataset are compared with manual segmentation results by two ophthalmologists and with the results of the method in some DME eyes, a collection of hard exudates exists which are imaged as intensely hyper-reflective structures. With regard to the evaluation of the proposed methods in subjects with these structures, we collected 2 subjects with these structures from the UMN eye clinic.

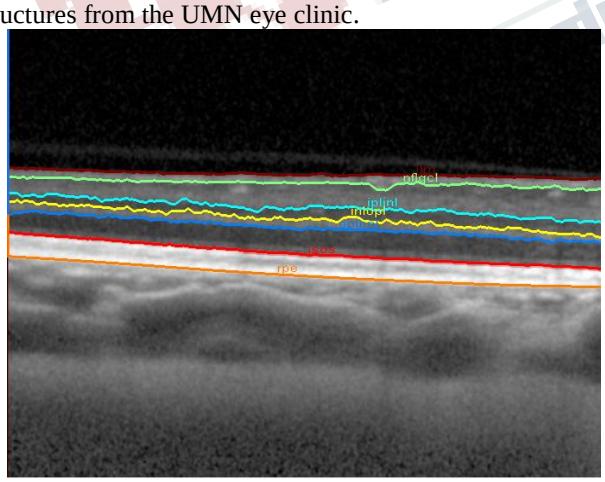

Figure 6.3 Fluid/cyst segment Region

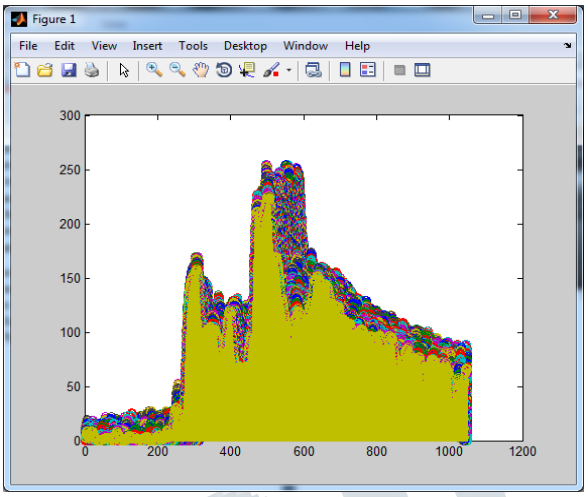

Figure 6.4 Fluid/cyst segment Region of Interest

V. CONCLUSION

These errors do not affect the final fluid/cyst segmentation results since segmented layers are just used in the ROI segmentation and post processing steps. In few images which are very dim, gradient information of the layer structures is almost lost and the OPL layer segmentation method follows a wrong path. This path may be even under the ISM layer. In these cases, the final fluid/cyst segmentation results will be affected and false positive pixels are segmented as fluid/cyst region which is due to the fact that in very dim images many pixels are similar to fluid/regions and the middle layer segmentation fails to ignore them in the post-processing step.

REFERENCES

[1] D. Huang, E. A. Swanson, C. P. Lin, J. S. Schuman, W. G. Stinson, W. Chang, M. R. Hee, T. Flotte, K. Gregory, C. A. Puliafito et al., "Optical coherence tomography," Science (New York, NY), vol. 254, no. 5035, p. 1178, 1991.

[2] R. Kafieh, H. Rabbani, M. D. Abramoff, and M. Sonka, "Intra-retinal layer segmentation of 3d optical coherence tomography using coarse grained diffusion map," Medical image analysis, vol. 17, no. 8, pp. 907–928, 2013.

[3] S. J. Chiu, M. J. Allingham, P. S. Mettu, S. W. Cousins, and J. A. Izatt, "Kernel regression based segmentation of optical coherence tomography images with diabetic macular edema," Biomedical optics express, vol. 6, no. 4, pp. 1172–1194, 2015.

[4] J. W. Yau, S. L. Rogers, R. Kawasaki, E. L. Lamoureux, J. W. Kowalski, T. Bek, S.-J. Chen, J. M. Dekker, A. Fletcher, and J. Grauslund, "Global prevalence and major risk factors of diabetic retinopathy," Diabetes care, vol. 35, no. 3, pp. 556–564, 2012.

[5] J. Pe'er, R. Folberg, A. Itin, H. Gnessin, I. Hemo, and E. Keshet, "Upregulated expression of vascular endothelial growth factor in proliferative diabetic retinopathy." British journal of ophthalmology, vol. 80, no. 3, pp. 241–245, 1996.

[6] D. C. DeBuc, A review of algorithms for segmentation of retinal image data using optical coherence tomography. INTECH Open Access
Publisher, 2011.

[7] F. Smarandache, A Unifying Field in Logics Neutrosophic Logic. Neutrosophy, Neutrosophic Set, Neutrosophic Probability. American Research Press, 2005.

[8] H.-D. Cheng and Y.Guo, "New Neutrosophic approach to image segmentation," in Pattern Recognition, vol. 42, no. 5, pp. 587–595, 2009.

[9] M. Zhang, L. Zhang, and H. Cheng, "A neutrosophic approach to image segmentation based on watershed method," Signal Processing, vol. 90, no. 5, pp. 1510–1517, 2010.

[10] A. Sengur and Y. Guo, "Color texture image segmentation based on neutrosophic set and wavelet transformation," Computer Vision and Image Understanding, vol. 115, no. 8, pp. 1134–1144, 2011.

[11] A. Heshmati, M. Gholami, and A. Rashno, "Scheme for unsupervised colour–texture image segmentation using neutrosophic set and nonsubsampled contourlet transform," IET Image Processing, vol. 10, no. 6, pp. 464–473, 2016.

[12] Y. Guo, A. S¸engur, and J. Ye, "A novel image thresholding algorithm¨ based on neutrosophic similarity score," Measurement, vol. 58, pp. 175– 186, 2014.

[13] J. Shan, H. Cheng, and Y. Wang, "A novel segmentation method for breast ultrasound images based on neutrosophic l-means clustering," Medical physics, vol. 39, no. 9, pp. 5669–5682, 2012.

[14] Y. Guo and A. S¸engur, "A novel image edge detection algorithm based¨ on neutrosophic set," Computers & Electrical Engineering, vol. 40, no. 8, pp. 3–25, 2014.

[15] Y. Guo and A. Sengur, "Ncm: Neutrosophic c-means clustering algorithm," Pattern Recognition, vol. 48, no. 8, pp. 2710–2724, 2015.

[16] B. Peng, L. Zhang, and D. Zhang, "A survey of graph theoretical approaches to image segmentation," Pattern Recognition, vol. 46, no. 3, pp. 1020–1038, 2013.

[17] M. K. Garvin, M. D. Abramoff, R. Kardon, S. R. Russell, X. Wu, and` M. Sonka, "Intraretinal layer segmentation of macular optical coherence tomography images using optimal 3-d graph search," IEEE transactions on medical imaging, vol. 27, no. 10, pp. 1495–1505, 2008.

[18] Q. Yang, C.A. Riesman. Wang,Y. Fukuma, ,M.Hangai, N. Yoshimura, A. Tomidokoro, M. Araie, A. S. Raza, D. C. Hood et al., "Automated layer segmentation of macular oct images using dual-scale gradient information," Optics express, vol. 18, no. 20, pp. 21293–21307,

[19] S. J. Chiu, X. T. Li, P. Nicholas, C. A. Toth, J. A. Izatt, and S. Farsiu, "Automatic segmentation of seven retinal layers in sdoct images congruent with expert manual segmentation," Optics express, vol. 18, no. 18, pp. 19413–19428, 2010.

[20] K. Lee, M. Niemeijer, M. K. Garvin, Y. H. Kwon, M. Sonka, and M. D. Abramoff, "Segmentation of the optic disc in 3-d oct scans of the optic nerve head," IEEE transactions on medical imaging, vol. 29, no. 1, pp. 159–168, 2010.

[21] S. J. Chiu, J. A. Izatt, R. V. O'Connell, K. P. Winter, C. A. Toth, and S. Farsiu, "Validated automatic segmentation of amd pathology including drusen and geographic atrophy in sd-oct images," Investigative ophthalmology & visual science, vol. 53, no. 1, pp. 53–61, 2012.

[22] K. K. Parhi, A. Rashno, B. Nazari, S. Sadri, H. Rabbani, P. Drayna, and D. D. Koozekanani, "Automated fluid/cyst segmentation: A quantitative assessment of diabetic macular edema," Investigative Ophthalmology & Visual Science, vol. 58, no. 8, pp. 4633–4633, 2017.